

Chapter 2

Nano-scale Force Spectroscopy Applied to Biological Samples

Sandor Kasas, Charles Roduit, and Giovanni Dietler

2.1 Introduction

The term force spectroscopy (FS), being widely used and somewhat broadly applied in the scientific community, can convey a rather misleading impression. In the framework of the present article, its use will be confined to the technique where measurements are made to study the behavior of a molecule or a system that is subjected to stretching or torsional forces. The number of published studies relating to this topic has notably increased during the recent years, a trend that reflects technical advancements in the means of manipulating single atoms or single molecules. FS is performed by applying a controlled pulling force to the molecule or system of interest. The force may be exerted optically [1], with magnetic tweezers [2], by the application of biomembrane force probes of hydrodynamic drag [3], via the mediation of fibers [4], or by the use of an atomic force microscope (AFM) [5]. The latter technique is the most commonly applied option. Consequently, this review will report mainly on AFM experiments. Similarly, since the vast majority of force-spectroscopy studies nowadays involve biological systems, these will be dealt in most detail.

Biological entities, from single proteins to whole organisms, are continuously exposed to mechanical stress. Consequently, numerous force-resisting structures have been developed during the course of evolution. The physical principles that underlie the mechanical functions of proteins are still a subject of intensive investigation. Fortunately, FS now offers us an opportunity of exploring and understanding the molecular basis of the different solutions that have been selected by evolution. AFM-based FS permits an exploration of biological assemblies on different scales. This review article will open with a short introduction to the forces that act on the molecular scale and this will be followed by a brief description of the

S. Kasas (✉)

Laboratoire de Physique de la Matière Vivante, EPFL, CH-1015 Lausanne, Switzerland
e-mail: sandor.kasas@epfl.ch

instrument and its working principles. Finally, FS experiments that have been conducted using systems of increasing complexities from single-molecule stretching to protein–plasmalemma interactions will be described.

2.2 Forces on the Molecular Scale

The smallest forces that act on a molecule are of entropic origin and are generated by thermal agitation. They represent the work that has to be undertaken to fully stretch a polymeric molecule without deforming its chemical bonds. This polymeric molecule spontaneously adopts a randomly coiled configuration, which maximizes its configurational entropy. These forces are rather weak and typically involve energies in the order of $k_B T$, where k_B is the Boltzman constant and T is the absolute temperature. Bond lengths in the order of a nanometer are typically implicated, and the resulting forces lie in the pN-range.

Noncovalent-interaction forces are stronger than the entropic ones and usually involve van der Waals, hydrogen, or ionic bonding. A single noncovalent interaction can be in the order of 10–100 pN. These are typically the forces that are needed to break most of the receptor–ligand bonds encountered in biology and to deform the internal structure of a molecule (e.g., secondary, tertiary, or quaternary structure of a protein).

Covalent bonds are the strongest forces encountered on the molecular scale, and they have a magnitude of approximately 1 nN. To deflect a typical AFM cantilever by 1 nm, a force of 60 pN must be applied to its end. Hence, depending upon the sensitivity of the instrument, all of the aforementioned forces lie within the measurable range of an AFM.

2.3 The Atomic Force Microscope

The AFM was invented in 1986 [6] for the imaging of samples, and it soon became popular among biologists. The reason thereof lies in the instrument’s potential to “observe”, with an unprecedented vertical and lateral resolution, biological systems that are immersed in a fluid (viz., under near-physiological conditions). The working principle of the instrument can be summarized as follows. A very sharp tip, which is fixed to the end of a cantilever, scans the sample. During the scanning, the interaction forces between the atoms of the sample and the atoms of the tip-end bend the cantilever. The vertical deflection of the cantilever is computationally correlated with the x and the y -coordinates of the tip to yield the three-dimensional topography of the sample. The tip and the cantilever are composed of silicon or silicon nitride and are available in different sizes and shapes and with different spring constants. Typically, the tips are pyramidal in shape with a base length of about 5 μm and an apical radial curvature of less than 15 nm. Cantilevers can have either a triangular or a rectangular form, with the longest-side lengths ranging from maximally 200 μm

down to 3 μm . Cantilevers with the smallest dimensions are used for high-speed AFM imaging. The vertical position of the tip is detected by a laser beam, which is reflected off the end of the cantilever. The beam terminates on a multi-segment photodiode (2 or 4 components), which converts the light intensity into a current. Variations in the illumination of the different segments of the photodiode are used by the controlling computer to calculate the tip's position along the z -axis. In most instruments, sample scanning beneath the tip is achieved using piezo electric crystals, which deforms in a predictable manner when exposed to a certain voltage. The scanning process can be achieved by different means. In some microscopes, the sample is moved in the x , y , and z -directions beneath an immobile tip. Instruments that are used for the observation of large samples and that are designed to be mounted above an inverted optical microscope are usually equipped with a tip that can be moved above an immobile sample. A combination of these two options has recently become available on the market: the sample is moved in the x and the y -directions, while the tip is displaced only along the z -axis. This configuration maximizes the scanning size and the displacement of the tip in the z -direction.

The feature that renders the instrument particularly interesting for biological applications is its capacity to operate equally well within vacuum, air, or fluid. By virtue of special injection systems, near-atomic resolution can be preserved even during the course of fluid exchange within the imaging chamber [7] (Fig. 2.1).

As aforementioned, the AFM was originally developed to map the topography of nonconducting samples. However, since 1992, the instrument has been shown to be capable of probing also the mechanical properties of a sample, or its affinity for

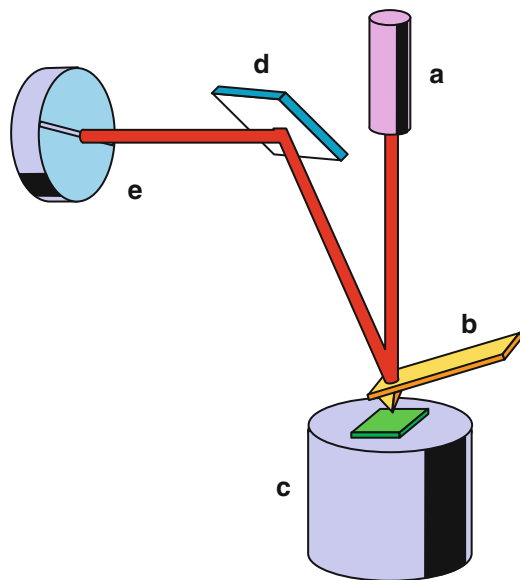


Fig. 2.1 The principal components of an AFM: (1) laser diode, (2) cantilever and tip, (3) piezo and sample (green), (4) mirror, (5) photodiode

tip-attached molecules. This type of measurement is achieved by recording and analyzing the so-called force–distance (FD) curves. These curves represent the deformation of the cantilever during its approach toward and its withdrawal from the sample. The mechanical properties of the sample are explored by pushing the tip into the sample, which causes its indentation, and recording the deformation of the cantilever during the process. If the sample is hard, the tip will not penetrate it, and the in-contact region of the FD curve will be a straight line with a slope of 45° . If the sample is soft, the tip will penetrate it, and the in-contact region of the FD curve will be flatter and of a more complex shape, which, in ideal cases, can be fitted to the Hertz model. This model predicts the shape of the FD curve for a sample that is flat, of infinite dimensions, isotropic, and homogeneous. For this mathematical modeling, the shape of the tip and the spring constant of the cantilever must be known. A comprehensive review of the factors that influence the shape of FD curves has been published by Cappella [8].

The affinity between the tip (or between any chemical species attached to it) and the sample can be deduced by careful examination of the retraction part of the FD curve. After making contact with the sample, the tip retracts, and if no link connects it to the sample, the cantilever recovers its resting position as soon the tip leaves the surface. However, if the tip (or the chemical species that coats it) interacts with the sample due to the existence of a strong attractive force or to the establishment of a molecular link between the tip and the sample, the cantilever is first deflected downwards. However, as soon as the retraction force of the cantilever exceeds the rupturing point of the newly formed bond, the cantilever recovers its resting position, which is maintained until the end of the FD curve.

If one knows the spring constant of the cantilever (viz., the constant that relates the deflection of the cantilever to the restoring force that it generates) and its deformation at the moment when the unbinding event occurs, then it is possible to calculate the force that is required to detach the tip from the surface or to break the bond between the tip-attached molecules and those on the surface of the sample (Fig. 2.2).

FD curves can be successively recorded all over the sample to yield a force–volume (FV) image. To this end, an FD curve is recorded for each pixel that composes the image. This type of imaging is extremely rich in information: a single FV file can furnish data respecting the topography of the sample, its stiffness as a function of depth, the position of a molecule of interest at its surface, and the interaction force between this molecule and those attached to the tip.

The potential of the AFM has been greatly exploited in recent years to gain an insight into numerous molecular phenomena in the fields of biology and biophysics, such as protein folding and ligand–receptor affinity. In the following sections, some of the domains in which the analysis of FD curves has significantly contributed to our understanding of the bio-nano world will be reviewed. Several other fields of investigation, which have been less successful to date, but are likely to benefit from future developments in nanotechnology, are also mentioned.

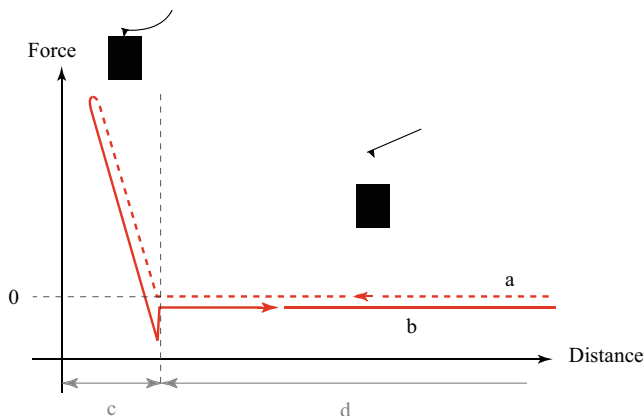


Fig. 2.2 Graph depicting the four relevant sections of a typical force–distance (FD) curve: (a) extension, (b) retraction, (c) in contact, (d) off-contact region

2.4 Unzipping and Stretching of DNA Molecules

Because of its profound importance to life, DNA has been more intensively studied than any other polymeric molecule. In living cells, certain proteins and drugs exert forces that can unzip and stretch DNA molecules. The development of instruments that permit the application of forces at a molecular level offers a unique opportunity of mimicking these physiological and pharmacological interactions. An understanding of the way in which proteins can exert DNA-deforming forces is of paramount importance in the fields of molecular biology, pharmacology, and polymer sciences. Furthermore, in recent years, several applications of DNA have been identified in the field of nanotechnology. These include its use as a molecular handle in single-molecule experiments [9], as a building block for the self-assembly of nanostructures [10], and as a base material for computing [11]. Hence, this field would also benefit from an improved knowledge of the physical properties of DNA.

Experiments that have been conducted to disclose the properties of DNA by applying forces to it can be essentially divided into two categories: those that pull the molecule along its axis, and those that unzip the molecule by pulling its two strands apart.

A study of the force-induced separation of double-stranded DNA is an important step toward understanding the processes of transcription and replication. The approach has been proposed as an alternative to the existing sequencing methods, since a sensitive force probe, such as optical tweezers [12] or an AFM [13], can accurately detect the binding strength between complementary base-pairs during the unzipping process. Krautbauer et al. used the AFM to sequence short DNA molecules with a resolution of 10 base-pairs. In these experiments, complementary molecules of single-stranded DNA were chemically attached to the AFM tip and to the substrate by their 5' and 3' ends, respectively. As the tip approached the substrate, complementary single strands came into

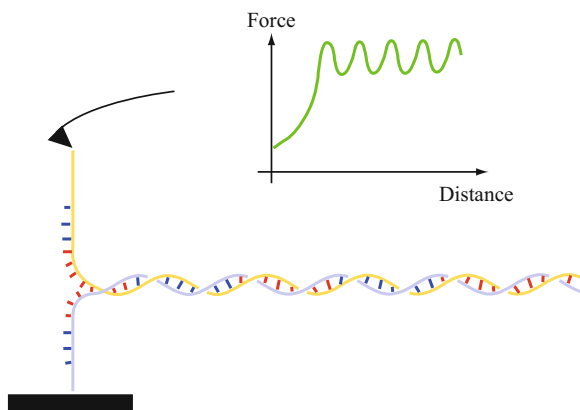


Fig. 2.3 Unzipping of complementary DNA oligonucleotides in the AFM (adapted from [13])

contact and double-stranded DNA was formed. As the tip was retracted from the substrate, the newly formed double strand was opened in a zipper-like fashion. The DNA sequence consisted of repeating blocks of 10 pure GC and 10 pure AT base-pairs. Since base-pairs of AT and GC are characterized by different pairing free energies (3.2 kT for AT and 5.2 kT for GC), the unzipping forces for the AT and the GC blocks should differ by approximately 5–10 pN over a stretch of about 20–25 nm. The experimental data confirmed this theoretical prediction (Fig. 2.3).

However, this technique suffers from the serious limitation that an ever-increasing amount of flexible, single-stranded DNA is created between the tip and the unzipping site. The stiffness of the single-stranded DNA thus rapidly dominates the FD curve, dramatically reducing the resolution of the instrument.

The stretching of double-stranded DNA along its axis can afford an insight into the stability and the phase transitions of the molecule. DNA is known to exist in different conformations, the B-form being the most common in living cells. However, if a force of about 65 pN is applied to the molecule, its contour length increases by a factor of 1.7, with the result that the B-form is converted into an over-stretched s-configuration [14–16].

Depending on which extremities of the DNA molecule are being pulled, the helical configuration is either conserved (if both 5' ends are pulled) or transformed into a ladder-like structure. By using an AFM to stretch different double-stranded DNA molecules, the B- to S-transition has been shown to depend upon the specific base-pairing in the double helix.

2.5 The Unfolding of Single Proteins

Proteins play a major role in all biological systems. Several of their functions are more or less directly related to their static structure and/or to their dynamics. Among the structural functions of proteins, conservation of the three-dimensional

shapes of cells and cellular rigidity via the cytoskeleton involving actin, tubulin, or intermediate filaments are the most obvious examples. Important dynamic functions include muscular contraction, vesicular transport in neuronal cells, and mechano-transduction in the inner ear. These functions are achieved by virtue of the particular molecular assemblies that permit proteins to resist deformation or to change their conformation under the influence of mechanical or chemical stimuli. Unveiling the subtle arrangements that underlie these functions is necessary to understand how biological systems operate and the reasons for their failure.

Knowledge about the atomic structure of a protein cannot throw any light on the constituents that are important for its mechanical properties. This information can be obtained only by applying a load to the protein and monitoring its pattern of deformation. Such experiments can be conducted using various tools, such as optical and magnetic tweezers. These devices can apply forces in the range of 1–100 pN to a single molecule. However, a survey of 7,500 proteins in a coarse-grained molecular-dynamics model has revealed that the unfolding forces lie between 0 and 350 pN [17]. The AFM operates precisely in this range of forces and is therefore the ideal (or at least a most appropriate) tool to monitor the behavior of proteins under force regimes that can unfold them completely and measure their changes in length at an Angstrom-level of resolution. Table 2.1 compares the specificities of various measurements made using optical tweezers, magnetic tweezers, and the AFM.

In a typical protein-unfolding experiment with the AFM, one end of the protein of interest is first attached to AFM tip of the instrument, and the other end is fixed to the substrate. Numerous techniques are available for anchoring the proteins to the AFM tip and to the substrate, a comprehensive overview of which has been published by Bizzarri and Cannistraro [18]. The measurement begins at the onset of tip retraction, which stretches the suspended segment of the protein. During its deflection downward, the cantilever applies a force to the protein, which is proportional to its vertical deflection. The first source of resistance to the extension is an entropic force, which tends to cause coiling up of the protein to maximize its disorder. Extension of the molecule reduces its entropy and produces a restoring force that bends the cantilever downwards. Knowing the spring constant of the cantilever, its deformation can be calibrated and translated into force.

Table 2.1 Comparison of the different specificities of single-molecule manipulation techniques (adapted from [50])

	Optical tweezers	Magnetic tweezers	AFM
Length scale	0.1–1,000 nm	10–10,000 nm	1–10,000 nm
Time scale	10^{-4} – 10^3 s	10^{-3} – 10^5 s	10^{-3} – 10^2 s
Force range	0.1–100 pN	0.005–20 pN	5–10,000 pN
Spatial resolution	0.1 nm	10 nm	0.5 nm
Limitations	Photo damage	Difficult to manipulate single molecules	Random-attachment geometries

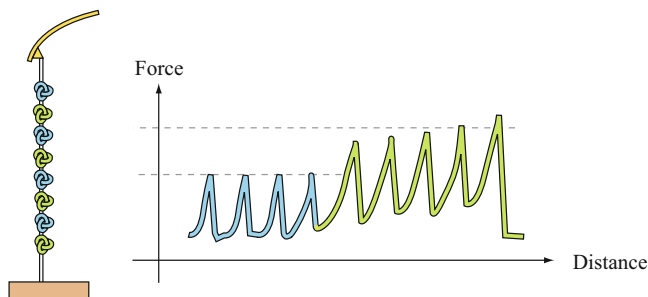


Fig. 2.4 Successive unfolding of the different domains of a heterodimeric polyprotein. The domains (depicted in *green* and *blue*) unfold according to their mechanical stability, irrespective of their order in the polyprotein (adapted from [49])

A further extension of the protein may cause an unfolding of some of its segments and an increase in its effective length. A sudden increase in the length of the protein causes a drop in the force acting on the cantilever and its return to the resting position. If the tip retraction continues and the protein contains other segments that can unfold, the process is repeated unless the protein breaks or detaches from the surface or the tip.

Figure 2.4 shows the saw-tooth extension curve of a polyprotein that is composed of four I27 and four I28 modules of human cardiac titin. The FD curve exhibits two levels of unfolding forces. Unfolding of the less stable I27 domains occurs at a force of approximately 200 pN and that of the more stable I28 ones at about 300 pN.

This technique can be used to study the unfolding of not only the single proteins but also the natural or synthesized polyproteins. In the latter situations, the technique permits an unambiguous identification of the parts of the polyprotein that are unfolding. Since an increase in the signal-to-noise ratio is possible, the amino acids can also be resolved. Furthermore, the technique renders possible an accurate module sizing of both the folded and the unfolded domains.

It is for this reason that the AFM is, nowadays, used to conduct force-spectroscopy experiments with heteropolyprotein constructs. An example of such an assembly is depicted in Fig. 2.5.

The first part of the construct embraces the protein of interest, while the second consists of identical, well-characterized domains, which serve as spacers and fingerprint the assembly (Ig/Fn domains in this specific case). The FD curve that is generated is depicted in the lower half of Fig. 2.5. The interpretation of FD curves is by no means a trivial undertaking and deserves a brief explanation.

2.5.1 Structural Basis for the Resistance to Unfolding

As aforementioned, when the force applied by the cantilever to the protein exceeds the entropic forces, then the naturally unfolded part of the protein can be assumed to

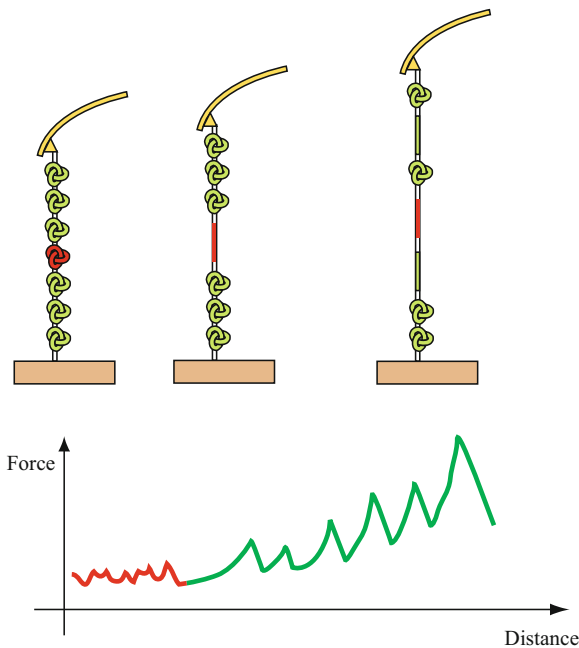


Fig. 2.5 The illustrated protein construct consists of five spacer domains (*blue*), which serves to fingerprint and furnish the domain of interest (*red*). The five evenly spaced contour-length increments, in *green*, are generated during the unfolding of the spacer domains, whereas the initial *red* path is generated by the domain of interest (adapted from [52])

be completely stretched. A characteristic unfolding then ensues, which leads to a sudden increase in the contour length of the protein and to a sharp drop in the acting force. The entropic elasticity of the unfolded portion of the protein can be formally described by different models, such as the freely jointed chain model [3], the freely rotating chain model [19], or the worm-like chain model [20]. The latter model is more widely implemented than any other option in the AFM community. It predicts that the stretch force (F) is related to the relative extension of the chain (x/L):

$$F(x) = \frac{kT}{A} \left(\frac{1}{4(1 - \frac{x}{L})^2} - \frac{1}{4} + \frac{x}{L} \right),$$

where A is the persistence length, which measures the chain's bending rigidity, k is the Boltzmann constant, T is the absolute temperature, x is the extension, and L is the contour length of the polypeptide. The contour length (L) increases after each unfolding event by an increment that equals the contour length in one of the folded domains.

Molecular-dynamics simulations reveal that the resistance of a protein to a force is determined principally by the topology of the molecule. Beta-sheets, in

which the hydrogen bonds are simultaneously loaded in a shear-geometry, appear to be more resistant to an externally applied force than the alpha-chains or mixtures of alpha-chains and beta-sheets [21]. However, recent studies have shown that even the load-resistance of beta-sheets is context-dependent and reflects other parts of the protein. It should also be borne in mind that rupture forces and extension lengths follow a distribution curve and that experimental parameters such as temperature [22] or the nature of the solvent [23] can influence the behavior of a protein. Pulling speed is also an important consideration in this type of measurement, and an increase in this parameter will give rise to an increase in the unfolding force [24]. This phenomenon will be discussed more fully later in this article, but a brief explanation is warranted here. An increase in the external force that is applied to a protein lowers the activation barrier between the folded and the unfolded states within the time-span of the experiment. Consequently, the thermal fluctuations exceed the unfolding barrier. The dependence of the unfolding forces on the force-loading rate can be used to estimate the unfolding rate constant, which represents the time that a domain needs to unfold spontaneously (i.e., in the absence of an external force). The unfolding rate constant can be calculated using Bell's model:

$$\alpha(F) = \alpha_0 \exp\left(\frac{F\Delta x}{kT}\right),$$

where α_0 represents the unfolding rate in the absence of an external force, F the applied force, and Δx the distance to the unfolding transition state.

The unfolding probability of a protein pulled at a constant speed can be calculated using Monte-Carlo simulations. These simulations reveal that unfolding must be viewed as a stochastic process in which the unfolding probability is close to zero in the absence of an external force and increases with an increase in the applied force level to a maximum (100%) at F_{\max} (the magnitude of which depends upon the pulling speed).

2.5.2 Influence of Pulling Geometry on Force-Spectroscopy Measurements

So far, we have assumed polyproteins to be pulled in a direction that is perpendicular to the surface of the substrate. But this may not always be the case, and it has thus been considered worthwhile to estimate the measuring error that would arise if the polyproteins were to be stretched at a different angle. Surprisingly, simple trigonometric calculations of this kind [25] have disclosed the error to be less than 1%.

However, this kind of error should not be confused with the errors that arise by varying the direction of the externally applied force relative to the orientation of

the polyprotein. Changes in this parameter can give rise to a much broader margin of error [26].

2.5.3 Force-Ramp and Force-Clamp Measurements

Thus far, we have considered only constant-velocity measurements, which involve pulling the protein at a constant speed until each of the various domains has unfolded. On the one hand, this type of measurement furnishes precise information relating to the end-to-end length of the polyprotein and to the positions of the different barriers. On the other hand, force ramping [27] and force clamping [28] involve feed-back loops to control the force that is applied to the molecule, thereby permitting an easier determination of the folding and the unfolding rates.

In force-clamp spectroscopy, the polyprotein is held at a constant stretching force. When a module of the protein unfolds, the global length increases and the force (viz., the deflection of the cantilever) drops to zero. Since the feed-back loop in this mode is programmed to keep the force constant, the tip moves rapidly upward until the polyprotein is again stretched at the programmed force. This cycle is repeated until each of the modules has unfolded or until the protein detaches from the surface or the tip. One of the advantages of this technique is that it permits a straightforward determination of the unfolding probability by fitting a single exponential to the length versus time curve (Fig. 2.6).

In force-ramp spectroscopy, a linearly increasing force is applied to the polyprotein by raising the tip at a predetermined, constant speed. When a module

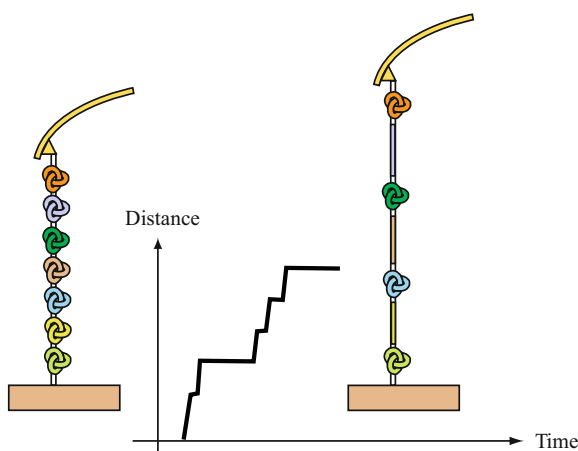
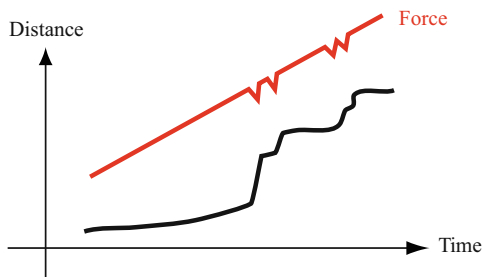


Fig. 2.6 Graph depicting a typical force-clamp measurement. The trace follows a characteristically staircase course, which reflects the stepwise unfolding of a single polyprotein (adapted from [37])

Fig. 2.7 Graph depicting a typical force-ramp measurement during the unfolding of a polypeptide (adapted from [37])



of the polypeptide unfolds, the retraction force drops to zero and the feed-back loop raises the tip rapidly until the force of the cantilever reaches the previous value. The linearly increasing force is then once again applied until another unfolding event occurs. The advantage of this technique is that it directly measures the unfolding probability as a function of the force that is applied to the protein (Fig. 2.7).

2.5.4 Refolding Studies

Force-clamp spectroscopy also permits monitoring of protein refolding at the single-molecule level. In experiments of this kind, the protein is first unfolded at a high force and then quenched at a lower one to permit refolding. Different types of protein such as ubiquitin [29], titin [30], and titin-like molecules [31] have been studied this way. Data gleaned from such experiments have revealed the different phases of the refolding process.

2.5.5 The Unfolding of Titin

To date, the AFM has been used to probe the force-spectroscopic characteristics of more than 50 different proteins. Notable examples include tenascin [32], spectrin [33], ubiquitin [34], and fibrinogen [35]. However, no protein has been more thoroughly investigated than titin. This circumstance is readily accounted for by the fact that titin is the largest known naturally occurring protein. It was also the first molecule to be investigated in FS by AFM [36]. Titin occurs within skeletal and cardiac muscle, radiating from the *z*-line to the center of a sarcomere. Its function can be likened to a spring that is charged to recoil the extended muscle fibers. The bulk of its mass is represented by an assemblage of globular domains, each of which is composed of immunoglobulin and fibronectin-type-III-like folds, and which are connected by elastin-like units.

Although several AFM studies have been performed using isolated molecules of native titin, most of the experiments have been conducted on recombinant, region-specific constructs. A comprehensive review of these investigations has been published by Linke and Grutzner (2008) [37].

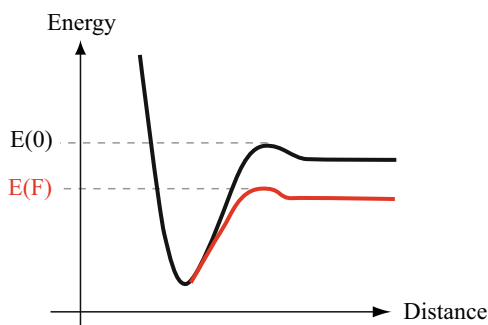
2.6 Measurement of Protein–Ligand Interactions

Protein–ligand interactions play a central role in biological processes. Recent developments in the AFM now render possible a direct quantification of the range and magnitude of the interactive forces operating between proteins and their ligands. Hitherto, interactions of this kind were essentially described in terms of the binding equilibrium, whereas now, they can be explored kinetically. This kinetic information is not only necessary to elucidate the molecular mechanism of the interaction, but is also important for the design of pharmacological agents.

Kinetic parameters that characterize protein–ligand interactions can be derived from FD curves. To understand the rationale of this methodology, one has to consider protein–ligand interaction as a molecular association with a limited lifetime. Even if no force is applied to pull the components of the complex apart, a spontaneous dissociation will be ultimately effected by thermal fluctuations. If the duration of the measurement exceeds the lifetime of the complex, then no unbinding event will occur. But if a constant stretching force is applied to the complex, its lifetime will be shortened, and it will dissociate more rapidly than it would in the absence of the force. The application of a force to the complex lowers its energy barrier, as depicted in Fig. 2.8.

The interaction force between a protein and its ligand depends greatly upon the manner in which the external force is applied during the course of an experiment, or, more precisely, upon the load rate, which is defined as the product of cantilever stiffness and pulling speed. Lowering of the loading rate results in lowering of the

Fig. 2.8 Graph depicting the energy barrier for the dissociation of a protein–ligand complex in the absence (*black line*) or presence (*red line*) of an externally applied force (adapted from [39])



interaction force. However, monitoring of unbinding force as a function of the loading rate is not in itself a useful measurement. Nevertheless, this information can be used to derive more meaningful thermodynamic and kinetic parameters, such as the kinetic off-rate (K_{off}), which affords an insight into the formation of bonds, their strength, and relaxation times. The kinetic off-rate is defined as:

$$K_{\text{off}}(F) = K_{\text{off}}(0) \left(\frac{F}{kT} \right),$$

where k is the Boltzmann constant, T is the absolute temperature, and kT is the thermal energy.

In practice, K_{off} is estimated by a first-order extrapolation of unbinding-force measurements that are recorded at different loading rates, since the unbinding force is usually linearly correlated with the logarithm of the loading rate.

If more than one barrier is involved, and if we assume that all barriers lie along a single one-dimensional escape path, then the curve follows a continuous sequence of linear regimes, as depicted in Fig. 2.9.

Using the AFM, loading rates ranging from 10 to 100 nN/s can be applied. Outside this range, hydrodynamic instabilities arise. The plotting of unbinding force against the logarithm of the loading rate permits an estimation of the dissociation rate at zero force [38].

The different steps that must be undertaken to estimate the K_{off} of a protein and ligand pair are represented in Fig. 2.10. Initially, the protein is attached to the tip and the ligand to the substrate (A), several thousand consecutive FD curves are then recorded at different loading rates (B). The unbinding events must be identified on the FD curves, and the corresponding unbinding force must be calculated. For each loading rate, a histogram is then constructed in which unbinding events is represented as a function of the force (C). These data are fitted to a Gaussian or Lorentzian curve to derive the value of the unbinding force for the protein–ligand pair. Finally, the logarithms of the most probable unbinding-forces values are plotted against the corresponding loading rate (D). The linear extrapolation of this curve gives the K_{off} -value.

Numerous protein–ligand unbinding experiments have been conducted in the AFM and a comprehensive review of this topic has been published by Lee et al.

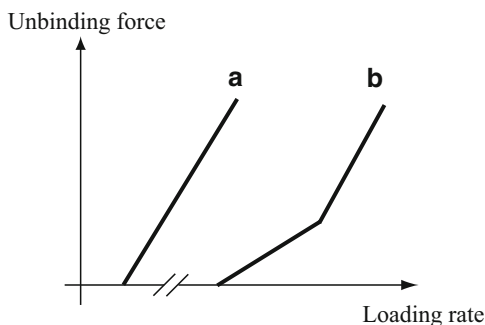


Fig. 2.9 Graphs depicting the relationship between the unbinding force and the logarithm of the loading rate for a molecule with a single energy barrier (**a**), and for one with two such barriers (**b**) (adapted from [39])

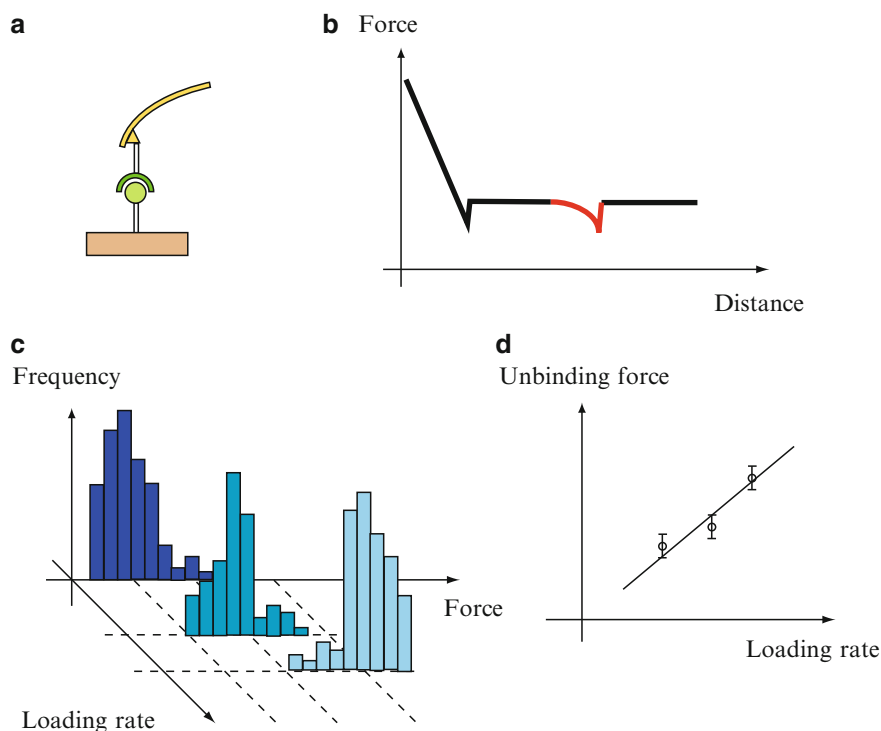


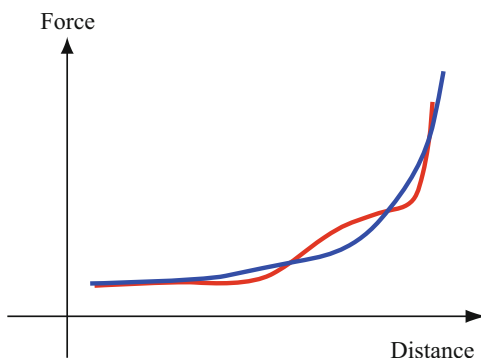
Fig. 2.10 Sequence of steps involved in deriving the K_{off} -value for a protein–ligand complex from measurements in the AFM (adapted from [39, 51])

(2007) [39]. One such study that is worth singling out here relates to the SNARE complex [40], which plays an important role in neurotransmission. It participates in the docking of neurotransmitter-filled vesicles and their fusion with presynaptic membranes. In the reported AFM experiments, the physiological system was simulated by anchoring some of the proteins onto the tip and several others onto the substrate. The interaction forces and the K_{offs} -values for the different proteins pairs that comprise the SNARE complex were calculated. Using these data, an estimate was made of the number of complexes that is required to securely attach a vesicle to the presynaptic membrane. The experimental set-up was also used to follow on-line the tetanus-toxin-induced disruption of the SNARE complex.

2.7 Stretching of Single Polysaccharides in the AFM

Polysaccharides have diverse and important functions in nature. They serve as building blocks in the construction of mechanically strong structures, as energy-storage molecules, and as recognition and signaling intermediates. To gain an

Fig. 2.11 Elasticity fingerprints of two linear polysaccharides (adapted from [43])



insight into the functional diversity of these molecules, it is necessary to analyze their structures. The primary structure of all polysaccharides comprises an arrangement of monosaccharides along the polymer chain. This mode of organization gives rise to a degree of structural diversity that is reputedly three orders of magnitude greater than is possible in proteins. Moreover, since the primary structure of polysaccharides is not encoded in genetic material, evolutionary changes therein cannot be effected as rapidly as with proteins.

Since 1997, AFM has been used to probe the elastic properties of single polysaccharide chains [41]. In the first experiments of this kind, chains of carboxymethylated dextran were mechanically stretched with a view to record the conformational changes in the C5–C6 bond of the glucose unit. Among the published studies, one in particular is worthy of mention here. It involved an attempt to identify the composition of polysaccharide samples by mechanically stretching individual, fluid-suspended molecules [42]. The FD curves that were collected during the course of these experiments differed according to the different shapes of the various length-normalized polysaccharides and could be used as fingerprints to identify single molecules (Fig. 2.11).

For reviews of investigations in which the AFM has been used to characterize the elastic properties of polysaccharides, the interested reader is referred to the publications of Sletmoen et al. [43] and Abu-Lail and Camesano [44].

2.8 Extraction of Surface Molecules

The methodology that is used to unfold single proteins can also be applied to extract proteins from the plasma membranes of living cells. In such experiments, the AFM tip is coated with covalent cross-linkers against the extracellular domains of the membrane proteins. When the tip approaches the cell, covalent bonds are formed

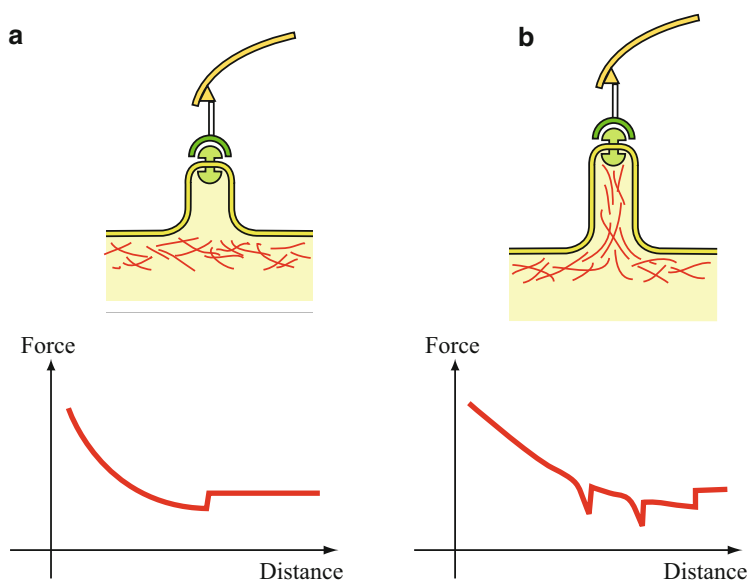


Fig. 2.12 Extraction of a plasmalemmal protein from a living cell, using the AFM (adapted from [53])

between the tip and the membrane proteins, and the maximal downward deflection of the cantilever during its retraction path yields information respecting the extraction force. Such experiments were conducted for the first time by Ikai and Afrin in 2002 [45]. The extraction force lay most frequently in the range of 400–600 pN, with little dependency on the loading rate. However, it should be borne in mind that to extract a protein from the plasmalemma of a living cell, first it is necessary to disrupt the hydrophobic bonds between the intramembranous portion of the protein and the surrounding phospholipids, and then to pull out its intracytoplasmic domain, which usually has a larger diameter than the intramembranous segment. Finally, it is necessary to rupture the noncovalent interactions between the cytoplasmic domain of the protein and submembranous components, such as the cytoskeleton as depicted on Fig. 2.12b.

2.9 Mapping of Surface-Membrane Molecules in Living Cells

If the AFM is programmed in such a way that the tip (or sample) is moved in the xy -plane after the acquisition of each set of FD curves, then it is possible to scan the surface of the sample and to map the distribution of individual receptors with a nanometric-scale resolution. The topography of the sample is resolved by

displaying the position of the tip as it contacts the sample (viz., by recording the point at which the cantilever begins the upward deflection that follows the tip-sample contact): such an image is depicted for a nerve cell in Fig. 2.13. During the retraction part of the FD curve, specific unbinding events can be topographically located. Typically, 16×16 or 32×32 FD curves are recorded for an area of a given size, and are then analyzed to extract information relating to parameters such as the tip-sample contact position and the location of binding–unbinding events between the functionalized tip and the surface receptors in the sample. This recognition imaging mode of the AFM has been successfully applied to erythrocytes and osteoblasts, as well as to vascular endothelial, ovary, and yeast cells. A comprehensive review of this topic has been published by Muller et al. [46].

Single-molecule mapping has been applied to reveal the distribution of fibronectin-attachment proteins (FAPs) on the surface of mycobacteria [47]. These proteins play an important role in the adhesion of bacteria and promote their binding to fibronectin within the extracellular matrix of the host. If FAPs were found to be homogeneously distributed over the surface of the bacterium under “physiological” conditions, then a dramatic change in this situation could be induced by the application of an antibiotic.

A similar methodology has also been used to localize glycosylphosphatidylinositol (GPI)-anchored proteins within the neurolemma of hippocampal neurons [48]. Although GPI-proteins are known to partition preferentially into cholesterol-rich micro domains, their mechanical properties and sizes are still under debate. By analyzing the in-contact region of FD curves, Roduit et al. were able to evaluate the mechanical properties of the cell membrane as well as the sizes and the stiffnesses of the microdomains. The image found in Fig. 2.13 simultaneously displays the topography of an axon, its variations in surface stiffness (coded in false colors), and the locations of GPI-anchored proteins.

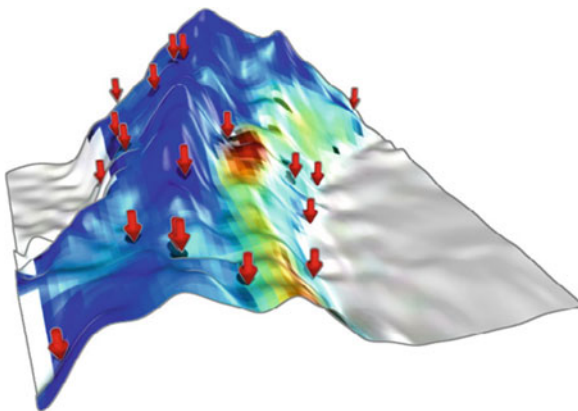


Fig. 2.13 AFM image of an axon, revealing its surface topography, variations in its surface stiffness (coded in *false colors*), and the locations of GPI-anchored neurolemmal proteins (*red arrows*)

2.10 Conclusion

In this article, the applications of the AFM to biologically relevant questions are briefly described. Biologically relevant systems that have been studied range from the single-molecule level to the cellular scale. The tool permits the investigation of the mechanical and elastic properties of proteins and of the kinetics of their interactions with ligands. By these means, it is now becoming possible to gain a truer insight into the relationships existing between biological activity and the physical properties of living matter.

References

1. Ashkin, A. (1980) Applications of laser-radiation pressure. *Science* 210: 1081–1088.
2. Amblard, F., B. Yurke, A. Pargellis, et al. (1996) A magnetic manipulator for studying local rheology and micromechanical properties of biological systems. *Review of Scientific Instruments* 67: 818–827.
3. Smith, S. B., L. Finzi and C. Bustamante (1992) Direct mechanical measurements of the elasticity of single DNA-molecules by using magnetic-beads. *Science* 258: 1122–1126.
4. Ishijima, A., T. Doi, K. Sakurada, et al. (1991) Sub-piconewton force fluctuations of actomyosin in vitro. *Nature* 352: 301–306.
5. Florin, E. L., V. T. Moy and H. E. Gaub (1994) Adhesion forces between individual ligand-receptorpairs. *Science* 264: 415–417.
6. Binnig, G., C. F. Quate and C. Gerber (1986) Atomic force microscopy. *Physical Review Letters* 56: 930–933.
7. Kasas, S., L. Alonso, P. Jacquet, et al. (2010) Microcontroller-driven fluid-injection system for atomic force microscopy. *Review of Scientific Instruments* 81.
8. Cappella, B. and G. Dietler (1999) Force-distance curves by atomic force microscopy. *Surface Science Reports* 34: 1–104.
9. EssevazRoulet, B., U. Bockelmann and F. Heslot (1997) Mechanical separation of the complementary strands of DNA. *Proceedings of the National Academy of Sciences of the United States of America* 94: 11935–11940.
10. Yan, H., S. H. Park, G. Finkelstein, et al. (2003) DNA-templated self-assembly of protein arrays and highly conductive nanowires. *Science* 301: 1882–1884.
11. Liu, Q. H., L. M. Wang, A. G. Frutos, et al. (2000) DNA computing on surfaces. *Nature* 403: 175–179.
12. Rief, M., H. Clausen-Schaumann and H. E. Gaub (1999) Sequence-dependent mechanics of single DNA molecules. *Nature Structural Biology* 6: 346–349.
13. Krautbauer, R., M. Rief and H. E. Gaub (2003) Unzipping DNA oligomers. *Nano Letters* 3: 493–496.
14. Cluzel, P., A. Lebrun, C. Heller, et al. (1996) DNA: an extensible molecule. *Science* 271: 792–794.
15. Smith, S.B., Y. Cui, and C. Bustamante (1996) Overstretching B-DNA: the elastic response of individual double-stranded and single-stranded DNA molecules. *Science* 271: 795–799.
16. Cocco, S., J. Yan, J. Léger, D. Chatenay and J.F. Marko (2004) Overstretching and force-driven strand separation of double-helix DNA. *Phys. Rev. E* 70: 011910.
17. Sulkowska, J. I. and M. Cieplak (2007) Mechanical stretching of proteins – a theoretical survey of the Protein Data Bank. *Journal of Physics-Condensed Matter* 19.

18. Bizzarri, A. R. and S. Cannistraro (2009) Atomic force spectroscopy in biological complex formation: strategies and perspectives. *Journal of Physical Chemistry B* 113: 16449–16464.
19. Livadaru, L., R. R. Netz and H. J. Kreuzer (2003) Stretching response of discrete semiflexible polymers. *Macromolecules* 36: 3732–3744.
20. Bustamante, C., J. F. Marko, E. D. Siggia, et al. (1994) Entropic elasticity of lambda-phage DNA. *Science* 265: 1599–1600.
21. West, D. K., D. J. Brockwell, P. D. Olmsted, et al. (2006) Mechanical resistance of proteins explained using simple molecular models. *Biophysical Journal* 90: 287–297.
22. Schlierf, M. and M. Rief (2005) Temperature softening of a protein in single-molecule experiments. *Journal of Molecular Biology* 354: 497–503.
23. Dougan, L., G. Feng, H. Lu, et al. (2008) Solvent molecules bridge the mechanical unfolding transition state of a protein. *Proceedings of the National Academy of Sciences of the United States of America* 105: 3185–3190.
24. Evans, E. and K. Ritchie (1997) Dynamic strength of molecular adhesion bonds. *Biophysical Journal* 72: 1541–1555.
25. Carrion-Vazquez, M., P. E. Marszalek, A. F. Oberhauser, et al. (1999) Atomic force microscopy captures length phenotypes in single proteins. *Proceedings of the National Academy of Sciences of the United States of America* 96: 11288–11292.
26. Brockwell, D. J., E. Paci, R. C. Zinober, et al. (2003) Pulling geometry defines the mechanical resistance of a beta-sheet protein. *Nature Structural Biology* 10: 731–737.
27. Marszalek, P. E., H. B. Li, A. F. Oberhauser, et al. (2002) Chair-boat transitions in single polysaccharide molecules observed with force-ramp AFM. *Proceedings of the National Academy of Sciences of the United States of America* 99: 4278–4283.
28. Oberhauser, A. F., P. K. Hansma, M. Carrion-Vazquez, et al. (2001) Stepwise unfolding of titin under force-clamp atomic force microscopy. *Proceedings of the National Academy of Sciences of the United States of America* 98: 468–472.
29. Fernandez, J. M. and H. B. Li (2004) Force-clamp spectroscopy monitors the folding trajectory of a single protein. *Science* 303: 1674–1678.
30. Garcia-Manyes, S., J. Brujic, C. L. Badilla, et al. (2007) Force-clamp spectroscopy of single-protein monomers reveals the individual unfolding and folding pathways of I27 and ubiquitin. *Biophysical Journal* 93: 2436–2446.
31. Bullard, B., T. Garcia, V. Benes, et al. (2006) The molecular elasticity of the insect flight muscle proteins projectin and kettin. *Proceedings of the National Academy of Sciences of the United States of America* 103: 4451–4456.
32. Cao, Y. and H. B. Li (2006) Single molecule force spectroscopy reveals a weakly populated microstate of the FnIII domains of tenascin. *Journal of Molecular Biology* 361: 372–381.
33. Rief, M., J. Pascual, M. Saraste, et al. (1999) Single molecule force spectroscopy of spectrin repeats: low unfolding forces in helix bundles. *Journal of Molecular Biology* 286: 553–561.
34. Brujic, J., R. I. Z. Hermans, S. Garcia-Manyes, et al. (2007) Dwell-time distribution analysis of polyprotein unfolding using force-clamp spectroscopy. *Biophysical Journal* 92: 2896–2903.
35. Brown, A. E. X., R. I. Litvinov, D. E. Discher, et al. (2007) Forced unfolding of coiled-coils in fibrinogen by single-molecule AFM. *Biophysical Journal* 92: L39–L41.
36. Rief, M., M. Gautel, F. Oesterheld, et al. (1997) Reversible unfolding of individual titin immunoglobulin domains by AFM. *Science* 276: 1109–1112.
37. Linke, W. A. and A. Grutzner (2008) Pulling single molecules of titin by AFM – recent advances and physiological implications. *Pflügers Archiv-European Journal of Physiology* 456: 101–115.
38. Schwesinger, F., R. Ros, T. Strunz, et al. (2000) Unbinding forces of single antibody-antigen complexes correlate with their thermal dissociation rates. *Proceedings of the National Academy of Sciences of the United States of America* 97: 9972–9977.
39. Lee, C. K., Y. M. Wang, L. S. Huang, et al. (2007) Atomic force microscopy: determination of unbinding force, off rate and energy barrier for protein-ligand interaction. *Micron* 38: 446–461.

40. Yersin, A., H. Hirling, P. Steiner, et al. (2003) Interactions between synaptic vesicle fusion proteins explored by atomic force microscopy. *Proceedings of the National Academy of Sciences of the United States of America* 100: 8736–8741.
41. Rief, M., F. Oesterhelt, B. Heymann, et al. (1997) Single molecule force spectroscopy on polysaccharides by atomic force microscopy. *Science* 275: 1295–1297.
42. Marszalek, P. E., H. B. Li and J. M. Fernandez (2001) Fingerprinting polysaccharides with single-molecule atomic force microscopy. *Nature Biotechnology* 19: 258–262.
43. Sletmoen, M., G. Maurstad, P. Sikorski, et al. (2003) Characterisation of bacterial polysaccharides: steps towards single-molecular studies. *Carbohydrate Research* 338: 2459–2475.
44. Abu-Lail, N. I. and T. A. Camesano (2003) Polysaccharide properties probed with atomic force microscopy. *Journal of Microscopy-Oxford* 212: 217–238.
45. Ikai, A., R. Afrin, A. Itoh, et al. (2002) Force measurements for membrane protein manipulation. *Colloids and Surfaces B-Biointerfaces* 23: 165–171.
46. Muller, D. J., M. Krieg, D. Alsteens, et al. (2009) New frontiers in atomic force microscopy: analyzing interactions from single-molecules to cells. *Current Opinion in Biotechnology* 20: 4–13.
47. Verbelen, C. and Y. F. Dufrene (2009) Direct measurement of Mycobacterium–fibronectin interactions. *Integrative Biology* 1: 296–300.
48. Roduit, C., G. van der Goot, P. de Los Rios, et al. (2008) Elastic Membrane Heterogeneity of Living Cells Revealed by Stiff Nanoscale Membrane Domains. *Biophysical Journal* 94: 1521–1532.
49. Carrion-Vazquez, M., A. F. Oberhauser, T. E. Fisher, et al. (2000) Mechanical design of proteins-studied by single-molecule force spectroscopy and protein engineering. *Progress in Biophysics and Molecular Biology* 74: 63–91.
50. Greenleaf, W. J., M. T. Woodside and S. M. Block (2007) High-resolution, single-molecule measurements of biomolecular motion. *Annual Review of Biophysics and Biomolecular Structure* 36: 171–190.
51. Ikai, A. and R. Afrin (2003) Toward mechanical manipulations of cell membranes and membrane proteins using an atomic force microscope – an invited review. *Cell Biochemistry and Biophysics* 39: 257–277.
52. Puchner, E. M. and H. E. Gaub (2009) Force and function: probing proteins with AFM-based force spectroscopy. *Current Opinion in Structural Biology* 19: 605–614.
53. Afrin, R. and A. Ikai (2006) Force profiles of protein pulling with or without cytoskeletal links studied by AFM. *Biochemical and Biophysical Research Communications* 348: 238–244.



<http://www.springer.com/978-1-4419-6168-6>

Nano-Bio-Sensing

Carrara, S. (Ed.)

2011, X, 248 p., Hardcover

ISBN: 978-1-4419-6168-6